Available online at www.sciencedirect.com
SCIENCE DIRECT
Journal of Power Sources 156 (2006) 244–252
JOURNAL OF POWER SOURCES
www.elsevier.com/locate/jpowsour

Numerical study of reactant gas transport phenomena and cell performance of proton exchange membrane fuel cells

Jer-Huan Jang [a], Wei-Mon Yan [b,*], Chinh-Chang Shih [a]

[a] *Department of Mechanical Engineering, Northern Taiwan Institute of, Science and Technology, Pei-To, Taipei, Taiwan 112, ROC*
[b] *Department of Mechatronic Engineering, Huafan University, Shih Ting, Taipei, Taiwan 22305, ROC*

Received 22 April 2005; received in revised form 6 June 2005; accepted 8 June 2005
Available online 29 August 2005

Abstract

A two-dimensional numerical model has been established to investigate the performance of the PEM fuel cells. Parameters used in the analysis include the porosity and thickness of the gas diffuser layer (GDL). Results show that increasing the porosity of gas diffusion layer causes the increasing of mass transfer of fuel and air and results in a higher reaction rate. Therefore, a better performance of the fuel cell and more fuel consumption rate are observed. It is also demonstrated that the performance of the fuel cell increases with a decrease in the thickness of gas diffusion layer. The effects of liquid water condensation and flow directions of fuel and air are also considered in this analysis. Predicted results show that the performance of the PEM fuel cell without consideration of liquid water effect is always higher than that with consideration of liquid water effect. In addition, the performance of fuel cell with co-flow pattern of fuel and air is larger than that with counter flow.

Keywords: PEM fuel cell; Gas diffuser layer; Porosity; Mass transfer

1. Introduction

The proton exchange membrane fuel cell (PEMFC) is considered as a most promising and environmental friendly alternative power source for both stationary and mobile applications due to its high efficiency and low operating temperature. Conventional PEMFCs operate on hydrogen as a fuel and oxygen or air as an oxidant to produce electricity, and heat and water are the major by-products. The gas streams have to be humidified to keep the membrane water swollen in order to obtain sufficiently high protonic conductivity. The reactant gases in the channel transport through the gas diffuser layer (GDL) and reach the catalyst layer to carry out electrochemical reaction. In past decades, substantial efforts have been focused on fuel cell structure design, development of catalyst, structure of catalyst and gas diffuser layer and the development of membrane with high performance, thermal and water management [1–8].

The performance of the fuel cell depends on the kinetics of the electrochemical process and performance of the components. Many experiments have been conducted by researchers for varying operating parameters. However, experimental investigations are costly. There are several models explain the mass transfer effect for different species in the fuel cell developed. The models can predict the cell performance precisely. Several mathematical modeling approaches have been proposed to describe the transport phenomena within PEMFCs and the impact of the water condensation on the cell performance. In recent year, two-dimensional models [9–12] were developed in order to investigate the distribution of gas components, water content of membrane, current density and net water transport along the flow channel. Gurau et al. [13] presented a comprehensive model for the entire sandwich of a PEMFC including the gas channels and considered the

* Corresponding author. Tel.: +886 2 26632102x4023; fax: +886 2 26632143.
E-mail address: wmyan@huafan.hfu.edu.tw (W.-M. Yan).

0378-7753/$ – see front matter © 2005 Elsevier B.V. All rights reserved.
doi:10.1016/j.jpowsour.2005.06.029

Nomenclature

Aj_0	reference exchange current density ($A\,m^{-2}$)
a	chemical activity of water vapor in cathode
C_F	quadratic drag factor
C	concentration
D	diffusivity ($m^2\,s^{-1}$)
F	Faraday constant, 96485 c mol^{-1}
i	current density ($A\,m^{-2}$)
j	current density ($A\,m^{-2}$)
k	permeability (m^2)
k_c	condensation rate constants
k_e	evaporation rate constants
M	molecular weight
P	pressure (atm)
P_i	partial pressure for i species (atm)
R	universal gas constant ($8.314\,J\,mol^{-1}\,K^{-1}$)
R_{VS}	volume-to-surface ratio of the porous material
s	the ratio of the volume of pore occupied by liquid water to the volume of pore in the porous medium
S	source term in momentum equation
S_c	source term of chemical reaction in the species concentration equation
S_j	source term in phase potential equation
S_L	source term with consideration of liquid water in the species concentration equation
t	thickness (m)
T	temperature (K)
U, V	velocities in the X and Y direction ($m\,s^{-1}$)
X, Y	rectangular coordinate system (m)
Z	number of electrons transferred
Z_f	charge transfer coefficient

Greek letters

α	charge transfer rate
ε	porosity
Φ	membrane potential
ν	kinematic viscosity ($m^2\,s^{-1}$)
σ	electric conductivity ($\Omega^{-1}\,m^{-1}$)
ρ	density ($kg\,m^{-3}$)
τ	tortuosity of the pore in the porous medium
η	overpotential

Superscripts

ref	reference value

Subscripts

a	quantity in anode
c	quantity in cathode
eff	effective value
g	of gas diffuser layer
H^+	for proton
H_2	for hydrogen
H_2O	for water
i	for i species
m	of membrane
O_2	for oxygen
sat	saturation pressure for water vapor
total	for total value
x	in the X direction
y	in the Y direction

gas-liquid phases in separate computation domains for transport in the gas distribution channels. It was assumed that the catalyst layer is infinitesimally thin. Hsing and Futerko [14] developed a two-dimensional model of coupled fluid flow, mass transport and electrochemistry of a PEMFC with taking into account the dependence of diffusion coefficient of liquid water in membrane. However, their model does not resolve catalyst layers and hence ignores the influence of spatial nonuniformity of water content on catalyst layer performance. Yi and Nguyen [15] proposed an along-the-channel model for evaluating the effects of various design and parameters on the performance of a PEMFC. The results show that the humidification of the anode gas is required to enhance the conductivity of the membrane, and the liquid injection and higher humidification temperature can improve the cell performance by introducing more water into the anode. It is noted that the mass transport processes in the presence of liquid water are not considered in these two-dimensional models.

In a typical PEMFC, the gas diffuser layers (GDLs) are required to have both reactant gases supply to the catalyst layer and water supply and removal in either vapor or liquid form. Although it is a seemingly minor component in a fuel cell, GDL is one of the important parts of the PEM fuel cell. Any change in the composition or the morphology of the GDL can lead to a substantial influence on fuel cell performance. Jordan et al. [16] experimentally examined the influence of diffusion-layer morphology on cell performance. They developed a model of the hydrophobilicity and porosity of the diffusion layer to explain the influence of the diffusion-layer morphology. Later, they [17] obtained results which showed that a low-porosity acetylene black enhances water removal from the membrane electrode assembly (MEA), and thus gives an improvement in gas-diffusion. Recently, Lee et al. [18] also studied experimentally the effect of the fabrication method and the thickness of the GDL on the cell performance. However, their focus was on the fabrication method, rolling, spraying and screen printing, of GDL effecting on the cell performance. Gurau et al. [19] proposed a mathematical model to obtain an analytic solution of the mass transport of reactant gas in a half-cell, in which the effects of the porosity and the tortuosity of the GDL and catalyst layer were explored due to the fact that the pores may be partially filed with liquid water. In their findings, the catalyst layer resistance at low current densities is equal to half

the value of the catalyst layer resistance corresponding to the limiting current density. Chu et al. [20] also used a half-cell model to investigate the effect of the change of the GDL on the performance of a PEMFC. They found that a fuel cell embedded with a GDL with a larger averaged porosity will consume a greater amount of oxygen, so that a higher current density is generated and a better fuel cell performance is obtained. Natarajan and Nguyen [21] developed a transient, two-dimensional mathematical model to study the effect of thickness of GDL for the cathode of a PEMFC. However, their model does not resolve the catalyst layer and water transport in the membrane is not considered. They found that the performance of the cathode was dominated by the dynamics of liquid water, especially in the high current density range, and a better performance can be observed when a thinner GDL is utilized in the fuel cell.

In the study of the PEMFCs, the water management is one of the most important issues. Nguyen and White [22] proposed a model of the water and heat management of the PEMFC systems, which includes the effect of electro-osmosis, diffusion of water, heat transfer from solid phase to gas phase and latent heat as water evaporation and condensation. They found that the ohmic loss is considerable at high current and the voltage loss is twice amount of that of the cathode electrode. Baschuk and Li [23] developed a mathematical model with variable degrees of water flooding in the PEMFC. Physical and electrochemical processes occurring in the membrane electrolyte, the cathode catalyst layer, the electrode backing layer and the flow channel were considered. They discovered that when the air was used as the cathode fuel, the flooding phenomena are similar at different operating conditions of the pressure and temperature comparing with experimental results. Wang et al. [24] have numerically modeled the two-phase flow and transport in the air cathode of PEMFCs. They found that the transport processes of liquid water and water vapor are affected by capillary effect and molecular diffusion, respectively. A two-dimension model was developed by Ge and Yi [25] to investigate the effects of operation conditions and membrane thickness on the water transport. In their study, the liquid water effect on the effective porosity for gas transport was considered to simplify the model of the two-phase flows in porous layers. The results revealed that the cell performance can be enhanced by increasing the cell temperature.

From the literatures reviews cited above, it is found that a full-cell mathematical model with consideration of catalyst layer and membrane water transport in a PEMFC has not been well examined yet. This motivates the present study. The objective of this work is to establish a two-dimensional, full-cell mathematical model with consideration of water saturation to investigate the effects of both the porosity and dimension of gas diffuser layer on the performance and gas transport phenomena of a PEMFC. Additionally, the effects of flow direction on the cell performance are taken into account in the analysis.

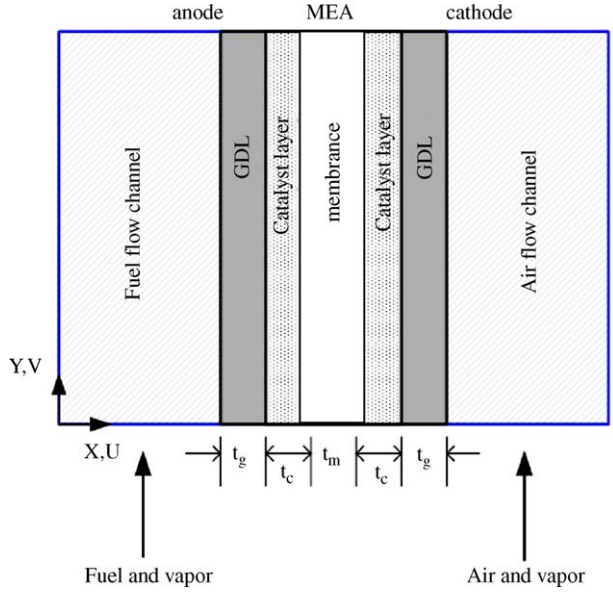

Fig. 1. Schematic diagram of complete PEMFC and coordinate system.

2. Analysis

The PEM fuel cell model described in this study is developed to investigate the effects of porosity and thickness of GDL. The computational domain includes a membrane sandwiched between two gas diffusion electrodes, and the flow channels of both anode and cathode. A schematic illustration of a PEMFC in the co-flow mode and associated coordinate system is shown in Fig. 1. U and V are the velocity components in the X and Y directions, respectively. The PEMFC in the counter-flow mode is also analyzed to study the performance of a PEMFC between co-flow and counter-flow modes for a comparison. Consequently, to simplify the problem, a steady state, two-dimensional, multi-species and along-the-channel model of a full-cell PEMFC is employed for the analysis. Four species were considered: hydrogen, oxygen, nitrogen and water vapor. Stationary conditions is assumed in this fuel cell, also the effect of gravity is neglected. It is assumed that the electrochemical reactions takes place only in the catalyst layer, and the gas mixtures in the flow channels are also considered to be perfect gases. Based on the definition of the Reynolds number and the velocity used in this work, the flow in the fuel cell is laminar. Therefore, all the transport equations were formulated for laminar behavior. The GDL, catalyst layer and PEM are assumed to be isotropically porous materials.

In the development of this numerical model of the PEM fuel cell as well as corresponding analyses, are crucial to gain a good understanding of the effect of GDL porosity and thickness on the cell potential. Most of the previous studies in this area have assumed for simplicity constant porosity of the GDL. This, however, does not reflect to the physical reality. Although it has been recognized that the performance of the fuel cell can be significantly influenced due to the porosity

variation, systematical studies are still rarely reported in the literature. In this study, porosity of GDL is chosen as 0.3, 0.4, 0.5 and 0.6. These values are chosen as closed as to the realistic situation and to reach a quantitative influence of GDL porosity on the cell performance.

2.1. Governing transport equations

According to the descriptions and assumption above, the basic transport equations for the two-dimensional PEM fuel cell are given as the following:

Continuity equation:

$$\frac{\partial U}{\partial X} + \frac{\partial V}{\partial Y} = 0 \tag{1}$$

Momentum equation:

$$U\frac{\partial U}{\partial X} + V\frac{\partial U}{\partial Y} = -\frac{1}{\rho}\frac{\partial P}{\partial X} + \nu\left(\frac{\partial^2 U}{\partial X^2} + \frac{\partial^2 U}{\partial Y^2}\right) + S_x \tag{2}$$

$$U\frac{\partial V}{\partial X} + V\frac{\partial V}{\partial Y} = -\frac{1}{\rho}\frac{\partial P}{\partial Y} + \nu\left(\frac{\partial^2 V}{\partial X^2} + \frac{\partial^2 V}{\partial Y^2}\right) + S_y \tag{3}$$

The source terms in Eqs. (2) and (3) are different in each computational domain due to the pressure difference when fluids pass through porous medium. So, the S_x and S_y in the GDL and the catalyst layer are:

$$S_x = -\frac{\nu\varepsilon_{\text{eff}}}{k}U - \frac{\varepsilon_{\text{eff}}^2 C_{\text{F}}\rho U}{\sqrt{k}}\sqrt{U^2+V^2} \tag{4}$$

$$S_y = -\frac{\nu\varepsilon_{\text{eff}}}{k}V - \frac{\varepsilon_{\text{eff}}^2 C_{\text{F}}\rho V}{\sqrt{k}}\sqrt{U^2+V^2} \tag{5}$$

and the S_x and S_y in the PEM are:

$$S_x = -\frac{\nu\varepsilon_{\text{eff}}}{k}U - \frac{\varepsilon_{\text{eff}}^2 C_{\text{F}}\rho U}{\sqrt{k}}\sqrt{U^2+V^2} + \frac{k}{\nu\varepsilon_{eff}} Z_{\text{f}} C_{\text{H}^+} F\cdot\nabla\Phi\cdot\frac{\partial U}{\partial X} \tag{6}$$

$$S_y = -\frac{\nu\varepsilon_{\text{eff}}}{k}V - \frac{\varepsilon_{\text{eff}}^2 C_{\text{F}}\rho V}{\sqrt{k}}\sqrt{U^2+V^2} + \frac{k}{\nu\varepsilon_{eff}} Z_{\text{f}} C_{\text{H}^+} F\cdot\nabla\Phi\cdot\frac{\partial V}{\partial Y} \tag{7}$$

where ε_{eff} is the effective porosity, C_{F} the quadratic drag factor and k is the permeability, Z_{f} the charge transfer coefficient, C_{H^+} the concentration of proton, F the Faraday constant and Φ is the membrane potential. In the analysis, Blake–Kozeny equation [26] is used to model k as below:

$$k = \left(\frac{D_{\text{IP}}^2}{150}\right)\left[\frac{\varepsilon_{\text{eff}}^3}{(1-\varepsilon_{\text{eff}})^2}\right] \tag{8}$$

and $D_{\text{IP}} = 6R_{\text{VS}}$, and R_{VS} is the volume-to-surface ratio of the porous material.

Species equation:

$$\varepsilon_{\text{eff}}\left(U\frac{\partial C_i}{\partial X} + V\frac{\partial C_i}{\partial Y}\right) = D_{i,\text{eff}}\left(\frac{\partial^2 C_i}{\partial X^2} + \frac{\partial^2 C_i}{\partial Y^2}\right) + S_{\text{c}} + S_{\text{L}} \tag{9}$$

where $D_{i,\text{eff}}$ is the effective diffusion coefficient of the i-th composition of fuel reactant. The effective diffusion coefficient is related to the diffusion coefficient in a nonporous system D_i by [27]:

$$D_{i,\text{eff}} = D_i\varepsilon_{\text{eff}}^{\tau} \tag{10}$$

where τ is the tortuosity of the pore in the porous medium, which is 1.5 for GDL and catalyst layer, and 6 for the membrane. S_{c} is the source term of chemical reaction in the species concentration equation, and is 0 in the gas flow channel and GDL. Furthermore, S_{c} is different with the reactant gases in the catalyst layer and PEM, e.g., S_{c} is $-\frac{j_{\text{a}}}{2FC_{\text{total,a}}}$ for hydrogen in catalyst layer, $-\frac{j_{\text{c}}}{4FC_{\text{total,c}}}$ for oxygen in catalyst layer, and $-\frac{j_{\text{c}}}{2FC_{\text{total,c}}}$ for water vapor in catalyst layer, and $\frac{ZF}{RT}D_{i,\text{ef}f,\text{H}^+}C_{\text{H}^+}\left(\frac{\partial^2\Phi}{\partial X^2} + \frac{\partial^2\Phi}{\partial Y^2}\right)$ in the PEM. The parameters j_{a} and j_{c} indicate the current density at the anode and cathode sides, respectively, and can be described by the following Butler–Volmer equations:

$$j_{\text{a}} = \text{Aj}_0^{\text{ref}}\left(\frac{C_{\text{H}_2}}{C_{\text{H}_2}^{\text{ref}}}\right)\left[\text{e}^{(\alpha_{\text{a}}F/RT)\eta} - \frac{1}{\text{e}^{(\alpha_{\text{c}}F/RT)\eta}}\right] \tag{11}$$

$$j_{\text{c}} = \text{Aj}_0^{\text{ref}}\left(\frac{C_{\text{O}_2}}{C_{\text{O}_2}^{\text{ref}}}\right)\left[\text{e}^{(\alpha_{\text{a}}F/RT)\eta} - \frac{1}{\text{e}^{(\alpha_{\text{c}}F/RT)\eta}}\right] \tag{12}$$

where Aj_0^{ref} is the exchange current density, α_{a} and α_{c} the electric charge transport rates in anode and cathode catalyst layers, η the overpotential, R the gas constant and T is the temperature of the fuel cell.

To consider liquid water effect in this work, a simplified two-phase model is used to describe the water transport in the PEM fuel cell. In this work, the liquid water effect is taken into account by modifying the mass diffusivity due to the liquid water filling the pores in the porous media and the liquid water generation in the species concentration equation. When the partial pressure of water vapor is greater than the saturation pressure of water vapor, the water vapor is assumed to condense and fill the pore in the porous media. The source term, S_{L} in the species concentration equation, Eq. (9), representing the quality of liquid water can be evaluated [28]:

$$S_{\text{L}} = \begin{cases} M_{\text{H}_2\text{O}}k_{\text{c}}\dfrac{\varepsilon_{\text{eff}}C_{\text{H}_2\text{O}}}{\rho RT}(P_{\text{H}_2\text{O}} - P_{\text{sat}}), & \text{if} \quad P_{\text{H}_2\text{O}} > P_{\text{sat}} \\ k_{\text{e}}\varepsilon_{\text{eff}}s(P_{\text{sat}} - P_{\text{H}_2\text{O}}), & \text{if} \quad P_{\text{H}_2\text{O}} < P_{\text{sat}} \end{cases} \tag{13}$$

where the M is the molecular weight and the k_{c} and k_{e} are the condensation and evaporation rate constants. The saturation

pressure of water can be expressed as:

$$P_{\text{sat}} = 10^{-2.1794+0.02953T-9.1837\times10^{-5}T^2+1.4454\times10^{-7}T^3} \tag{14}$$

It should be noted that the assumption of isothermal condition is utilized in this analysis to simplify the model. However, the saturation of water is greatly affected by the temperature in the fuel cell, such as the saturation pressure in Eq. (14). Nevertheless, when a single cell is tested, the cell temperature is usually controlled using heating rods and thermocouples. As a result, the operation temperature of a single fuel cell can be kept almost constant in all the regions of the working fuel cell. The temperature difference is small enough during cell operation that the assumption of isothermal condition is appropriate for the analysis.

In addition, the saturation, s, is defined as the ratio of the volume of pore occupied by liquid water to the volume of pore in the porous medium, then the effective porosity of porous media is modified to account the liquid water effect:

$$\varepsilon_{\text{eff}} = \varepsilon(1-s) \tag{15}$$

In order to evaluate the distributions of the local current density, the phase potential equation should be solved:

$$\frac{\partial}{\partial X}\left(\sigma_{\text{m}}\frac{\partial \Phi}{\partial X}\right) + \frac{\partial}{\partial Y}\left(\sigma_{\text{m}}\frac{\partial \Phi}{\partial Y}\right) = S_{\text{j}} \tag{16}$$

where $S_{\text{j}} = -j_{\text{a}}$ in the anode, $-j_{\text{c}}$ in the cathode and 0 in the membrane; σ_{m} is the electric conductivity of the membrane which can be calculated by the equation developed by Springer et al. [29]:

$$\sigma_{\text{m}}(T) = \sigma_{\text{m}}^{\text{ref}} \exp\left[1268\left(\frac{1}{303}-\frac{1}{T}\right)\right] \tag{17}$$

and the reference electric conductivity is:

$$\sigma_{\text{m}}^{\text{ref}} = 0.005139\lambda - 0.00326 \tag{18}$$

$$\lambda = \begin{cases} 0.043 + 17.81a - 39.85a^2 + 36.0a^3, & 0 \le a \le 1 \\ 14 + 1.4(a-1), & 1 < a \le 3 \end{cases} \tag{19}$$

In Eq. (19), the a is the ability of water vapor at the cathode side. Using the following relations between the phase potential Φ and current density I:

$$i_x = -\sigma_{\text{m}}\frac{\partial \Phi}{\partial x} \tag{20}$$

$$i_y = -\sigma_{\text{m}}\frac{\partial \Phi}{\partial y} \tag{21}$$

Eq. (16) can then be reduced to be:

$$\frac{\partial i_x}{\partial X} + \frac{\partial i_y}{\partial Y} = j_{\text{a}}, \quad \text{at anode} \tag{22}$$

$$\frac{\partial i_x}{\partial X} + \frac{\partial i_y}{\partial Y} = j_{\text{c}}, \quad \text{at cathode} \tag{23}$$

2.2. Boundary conditions

Boundary conditions for the dependent variables of the transport equations at the interfaces between different layers of the same domain are not required. At the gas channel outlet, the fully developed flow conditions are assumed:

$$U = \frac{\partial V}{\partial Y} = \frac{\partial C_i}{\partial Y} = 0 \tag{24}$$

The boundary conditions at the gas flow channel walls are:

$$U = V = \frac{\partial C_i}{\partial X} = 0 \tag{25}$$

In practical situation, the physical properties and their gradients are continuous on the interface. So the natural boundary conditions on the interface are the same velocity, same concentration and the same gradients. At the interfaces between the gas diffusers and the gas channels, the following boundary conditions are used:

$$\varepsilon_{\text{eff},X^+}\left.\frac{\partial V}{\partial X}\right|_{X=X^+} = \left.\frac{\partial V}{\partial X}\right|_{X=X^-}, \quad V_{X=X^+} = V_{X=X^-} \tag{26}$$

$$\varepsilon_{\text{eff},X^+}\left.\frac{\partial C_i}{\partial X}\right|_{X=X_1^+} = \left.\frac{\partial C_i}{\partial X}\right|_{X=X_1^-}, \quad C_{i,X=X^+} = C_{i,X=X^-} \tag{27}$$

The similar conditions are employed for the interfaces between the gas diffusers and the catalyst layers and the interfaces between the catalyst layers and membrane can be expressed as follows:

$$\varepsilon_{\text{eff},X^+}\left.\frac{\partial V}{\partial X}\right|_{X=X^+} = \varepsilon_{\text{eff},X^-}\left.\frac{\partial V}{\partial X}\right|_{X=X^-}, \quad V_{X=X^+} = V_{X=X^-} \tag{28}$$

$$\varepsilon_{\text{eff},X^+}\left.\frac{\partial C_i}{\partial X}\right|_{X=X^+} = \varepsilon_{\text{eff},X^-}\left.\frac{\partial C_i}{\partial X}\right|_{X=X^-},$$
$$C_{i,X=X^+} = C_{i,X=X^-} \tag{29}$$

The boundary conditions for the phase potential at the interface between the catalyst layer and the membrane are $\Phi = 0$ at the anode side, and $\frac{\partial \Phi}{\partial X} = 0$ at the cathode side. Because the phase potential is a linear distribution in the membrane, the phase potential boundary condition can be written as $\frac{\partial \Phi}{\partial Y} = 0$.

3. Numerical method

The solution to the governing equations is performed using a finite volume scheme by dividing the model domain into a number of cells as control volumes. In the finite volume method, the governing equations are numerically integrated over each of these computational cells or control volumes. The finite volume method exploits a collocated cell-centered

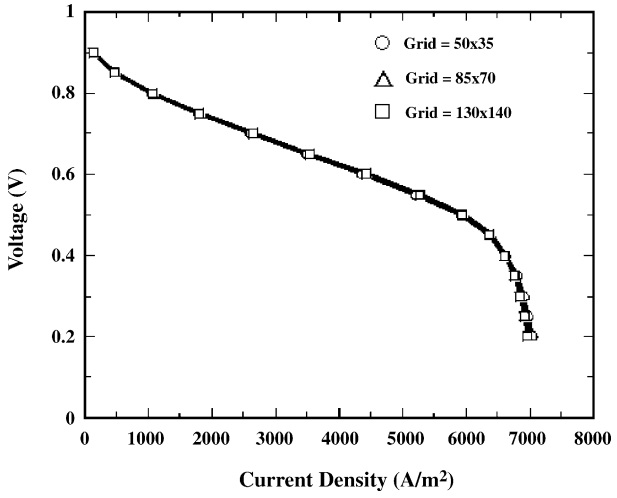

Fig. 2. Comparison of predictions for various grid systems.

variable arrangement, that implies all the dependent variables and material properties are stored at the cell center. The average value of any quantity within a control volume is given by its value at the cell center.

The governing equations can be expressed in the form of a generalized transport equation:

$$\nabla \cdot (\rho \vec{u} \phi - \Gamma_\phi \nabla \phi) = S_\phi \tag{30}$$

where ϕ denotes the general dependent variable, Γ_ϕ the exchange coefficient, S_ϕ the source term, $\vec{u}$ the velocity vector and ρ is the density. With the discritization of the governing equations, the coupled finite-difference equations can be expressed in the form of:

$$a_P \phi_P = a_E \phi_E + a_W \phi_W + a_N \phi_N + a_S \phi_S + S_\phi \tag{31}$$

where ϕ_P is the value of ϕ at the current point P, $\phi_E \ldots \phi_S$ stand for the values of the grid points adjacent to the point P and $a_p \ldots a_s$ are known as the link coefficients.

In this work, the non-uniform grid system of 85×70 is employed for the analysis. In order to examine the grid independence of the predictions, coarse and fine grid systems are considered in the preliminary tests. Effects of the grid number on the predictions of local current density are shown in Fig. 2. The maximum deviations among the computations on the grids of 50×35, 85×70 and 130×140 are less than 3%. Therefore, the grid system of 85×70 points seems to be sufficient to resolve the behaviors of the reactant gas transport in the present PEMFC model.

4. Results and discussions

In this work, the inlet conditions for anode and cathode are that the velocity is 1 m s^{-1}, the temperature is 333.15 K, and the relative humidity is 100%. The total length of the flow channel is 14 cm, and the cross-section of the flow channel is 1 mm × 1 mm. The thickness of the catalyst layer is taken to be 0.0000287 m. Results are obtained for cases presented in Table 1, where case 2 is the typical case for comparison.

Table 1
Values of the major parameters

	t_g (m)	ε_g	t_m (m)	Flow direction
1	0.0004	0.3	0.00175	Co-flow and counter-flow
2	0.0004	0.4	0.00175	Co-flow and counter-flow
3	0.0004	0.5	0.00175	Co-flow and counter-flow
4	0.0004	0.6	0.00175	Co-flow and counter-flow
5	0.0002	0.4	0.00175	Co-flow
6	0.0006	0.4	0.00175	Co-flow

4.1. Effect of GDL porosity

In order to study the effect of gas diffuser layer (GDL) porosity on the cell performance, Fig. 3 shows the polarization (*I–V*) curves with various GDL porosity of a fuel cell. For comparison, the results without liquid water effects in the model are also presented. An overall inspection on Fig. 3 discloses that the effect of the GDL porosity on the cell performance is negligibly small at the condition of high operating voltages. However, under low operating voltage conditions, the GDL porosity shows a significant influence on the *I–V* curves. In addition, the cell performance is increased with an increase in the GDL porosity with/without consideration of liquid water effect. This is because more reactant gases transfer into the catalyst layer with a higher GDL porosity, which in turns, more chemical reaction occurs and more reactant gases consume, which results in a better cell performance. It is also observed that the cell performance is over-predicted when the liquid water effect is not taken into account in the modeling. This maybe due to the fact that the void in GDL is filled with the liquid water, which in turn causes the reduction of mass transfer. It is also noted in Fig. 3 that the deviations in the cell performance between the results with and without consideration of liquid water effects are small at high operat-

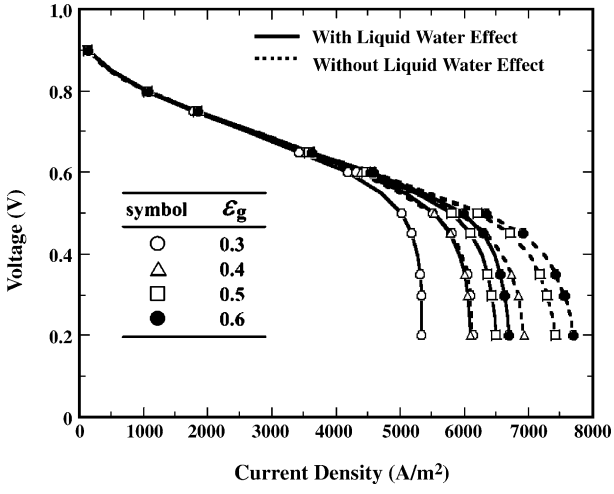

Fig. 3. Effects of GDL porosity on the polarization curves of the PEMFC with/without liquid water effects.

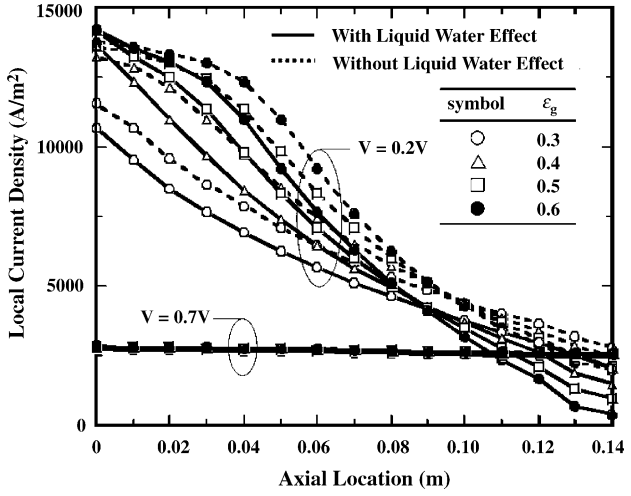

Fig. 4. Effects of GDL porosity on the local current density.

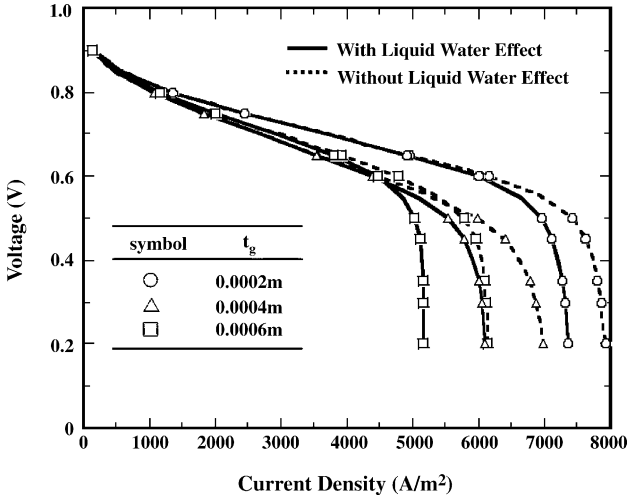

Fig. 5. Effects of GDL thickness on the polarization curves of the PEMFC with/without liquid water effects.

ing voltage conditions. This indicates that the fuel transport in the PEMFC can be treated as gas phase at high voltage conditions. However, at low voltage conditions, the liquid water effects on the cell performance are remarkable and cannot be neglected in the modeling. This confirms the fact that the mass transports at lower operating conditions are significant and, in turn, more water is generated in the catalyst layer of the cathode side. Therefore, two-phase flow effects should be considered under low operating voltage conditions.

It is shown from above that the GDL porosity has a remarkable impact on the cell performance. It is necessary to investigate the GDL porosity effect on the local transport characteristics of the PEMFCs. The GDL porosity effects on the local current density distributions at V = 0.7 and 0.2 V are presented in Fig. 4. To investigate the liquid water effects, the results with and without considerations of liquid water in the modeling are both presented in Fig. 4. The local current density decreases with the axial direction and is kept at almost the same low value under a higher operating voltage. It is expected that for the lower operating voltage, the electrochemical reaction is stronger in the catalyst layer. Therefore, the fuel is consumed in a higher rate when the fuel flows along the main flow direction, which in turn, causes the substantial variations in the local current density. A higher local current density is noted for the PEM fuel cell with a higher GDL porosity near the entrance. This indicates that an increase in GDL porosity enhances the diffusion transport of the reactant gas through the porous layers and, in turn, increases the local current density. However, at the downstream region, the current density decreases as the GDL porosity increases. The degradation in local current density in the downstream region is a reflection of the more efficient fuel transport and the chemical reaction in the upstream. Besides, the predictions reveal that the consideration of the liquid water in the simulation leads to the relatively lower current density than those in the cases without liquid water effect.

4.2. Effect of GDL thickness

The effect of the gas diffuser layer (GDL) thickness on the polarization curves of a PEM fuel cell is shown in Fig. 5. It is obvious that the cell performance with/without liquid water effect increases as the GDL thickness decreases, especially at lower operating voltage conditions. This is due to the increase of concentration gradient with a thinner GDL, which in turn, results in a higher mass transfer to the catalyst layer. Therefore, a larger current density takes place. However, it does not show the same trend at higher operating conditions ($V > 0.6$ V). Since the effects of the GDL thickness show a significant impact on the cell performance, the effect of GDL thickness on the local transport characteristic is also studied. Fig. 6 depicts the effect of the GDL thickness on the local current density along the axial direction at $V = 0.7$ and 0.2 V. It is clearly seen that the local current density for $V = 0.2$ V increases as the GDL thickness decreases, and

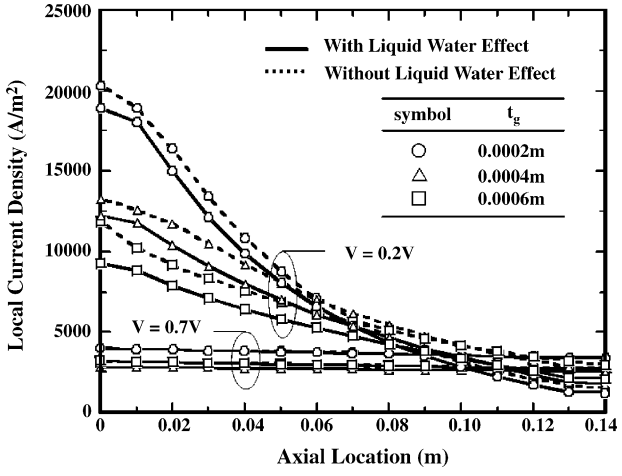

Fig. 6. Effects of GDL thickness on the local current density.

decreases along the axial direction. Nevertheless, the local current density for $V = 0.7$ V remains as a constant and do not show the same trend as that for $V = 0.2$ V as mentioned previously. It should be noted that the model used in this analysis is isothermal and single phase condition, the temperature gradient effect of the GDL and two-phase condition on the GDL shall be discussed in the future work. Since some have shown a thinner GDL is more easily flooded due to lower storage of liquid, thus performance under 2-phase conditions is better for a thicker GDL. Also, temperature gradient effects of the GDL are very important as well as electron transport.

4.3. Effect of flow direction

In this study, the effects of flow direction of reactant fuels in both the anode and cathode sides on the cell performance are also investigated. Fig. 7 represents the effects of the GDL porosity on the cell performance with the reactant fuels flowing in anode and cathode sides being co-flow and counter-flow conditions. It is obvious from Fig. 7 that the cell performance increases as the GDL porosity increases for the counter-flow condition. It is also noted that the cell performance with counter-flow condition is better at higher operating voltage conditions, while the cell performance with co-flow condition is better at lower operating voltage conditions. This is due to the remaining fuel reacts with air under higher operating voltage conditions with counter-flow condition, which results in a better cell performance. This phenomenon can be confirmed by the effects of flow direction of the reactant fuels on the local current density. Fig. 8 presents the distributions of the local current density along the axial direction with counter-flow condition for four GDL porosities at $V = 0.7$ and 0.2 V. Comparison of the corresponding results in Fig. 4 and Fig. 8 indicates that the local current density with counter-flow condition is higher than that with co-flow condition at $V = 0.7$ V. Besides, the local current density with counter-flow condition at $V = 0.2$ V is higher near the entrance. However, the local current density with co-flow condition becomes higher than that with counter-flow condition at the downstream ($Y > 0.03$ m). Because the electrochemical reaction rate is high under lower operating voltage conditions, the fuel consumption rate increases near the entrance with counter-flow condition, which in turn, causes the increase in local current density and less fuel along the axial direction.

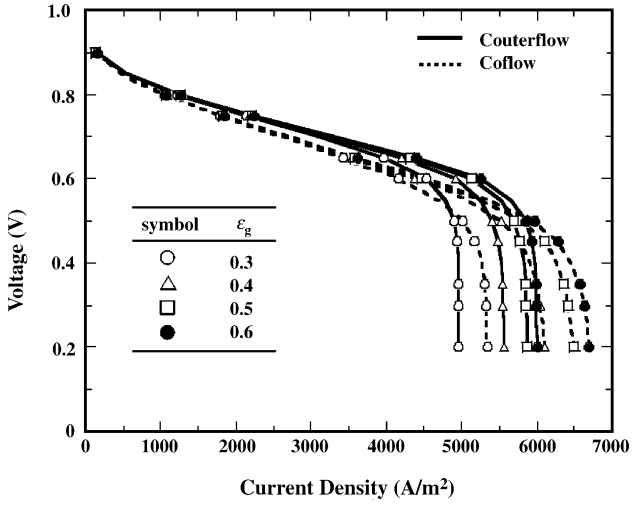

Fig. 7. Effects of flow direction of reactant fuels in both the anode and cathode sides on the polarization curves of the PEMFC.

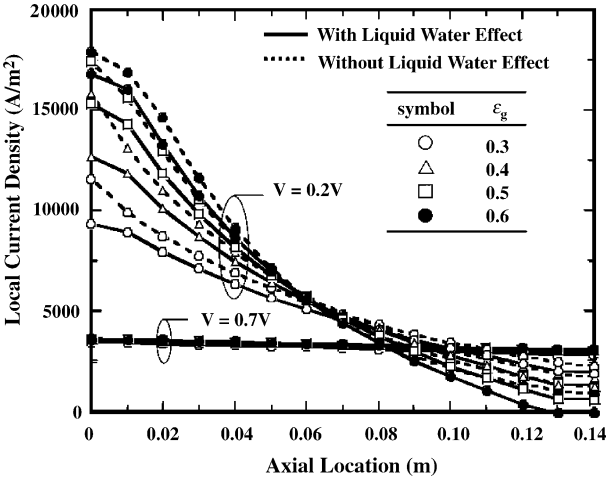

Fig. 8. Effects of GDL porosity on the local current density with counter-flow condition of reactant fuels in both the anode and cathode sides.

5. Conclusion

A steady, a two-dimensional, isothermal, multi-species, full-cell numerical model to analyze the performance of PEMFCs has been established. Liquid water effects were considered in this work. The effects of GDL porosity, membrane thickness, GDL thickness and flow direction of reactant fuels on the reactant gas transport and the cell performance are examined in detail. Brief summaries of the major results are listed in the following:

1. The cell performance is enhanced as the GDL porosity increases with/without consideration of liquid water effect. This is because more reactant gases transfer into the catalyst layer with higher GDL porosities, which in turns, more chemical reaction occurs and more reactant gases consume, and a better performance for the fuel cell is obtained.
2. The cell performance increases with a decrease in GDL thickness at lower operating voltage conditions. This is due to the fact that higher concentration gradients are resulted from the decrease in the GDL thickness, which in turns, results in a higher mass transfer to the catalyst layer and then more electrochemical reaction occurs.
3. The cell performance with counter-flow condition is higher at a higher operating voltage condition, while the

cell performance with co-flow condition is higher at a lower operating voltage condition.

Acknowledgements

The authors would like to acknowledge the financial support of this work by the National Science Council, ROC through the Contract NSC92-2212-E-211-001. The financial support from Northern Taiwan Institute of Science and Technology is also acknowledged.

References

[1] P. Costamagna, S. Srinivasan, Quantum jumps in the PEMFC science and technology from the 1960s to the year 2000. Part I. Fundamental scientific aspects, J. Power Sources 102 (2001) 242–252.
[2] P. Costamagna, S. Srinivasan, Quantum jumps in the PEMFC science and technology from the 1960s to the year 2000. Part II. Engineering, technology development and application aspects, J. Power Sources 102 (2001) 253–269.
[3] D.M. Bernardi, M.W. Verbrugge, Mathematical model of a gas diffusion electrode bonded to a polymer electrolyte, AIChE J. 37 (1991) 1151–1163.
[4] T.F. Fuller, J. Newman, Water and thermal management in solid-polymer-electrolyte fuel cells, J. Electrochem. Soc. 140 (1993) 1218–1225.
[5] W.M. Yan, C.Y. Soong, F. Chen, H.S. Chu, Effects of flow distributor geometry and diffusion layer porosity on reactant gas transport and performance of porton exchange membrane fuel cell, J. Power Sources 125 (2004) 27–39.
[6] F. Chen, Y.Z. Wen, H.S. Chu, W.M. Yan, C.Y. Soong, Convenient two-dimensional model for design of fuel channels for proton exchange membrane fuel cell, J. Power Sources 128 (2004) 125–134.
[7] T.V. Nguyen, A gas distributor design for proton-exchange-member fuel cells, J. Electrochem. Soc. 143 (1996) L103–L105.
[8] A.S. Arico, P. Creti, V. Baglio, E. Modica, V. Antonucci, Influence of flow field design on performance of a direct methanol fuel cell, J. Power Sources 91 (2000) 202–209.
[9] D. Singh, D.M. Lu, N. Djilali, A two-dimensional analysis of mass transport in proton exchange membrane fuel cells, Int. J. Eng. Sci. 37 (1999) 431–452.
[10] S. Um, C.Y. Wang, K.S. Chen, Computational fluid dynamics modeling of proton exchange membrane fuel cells, J. Electrochem. Soc. 147 (2000) 4485–4493.
[11] W. He, J.S. Yi, T.V. Nhuyen, Two-phase flow model of the cathode of PEM fuel cells using interdigitated flow fields, AIChE J. 46 (2000) 2053–2064.
[12] A.C. West, Influence of rib spacing in proton-exchange membrane electrode assemblies, J Appl. Electrochem. 26 (1996) 557–565.
[13] V. Gurau, H. Liu, S. Kakac, Two-dimensional model for proton exchange membrane fuel cells, AIChE J. 44 (1998) 2410–2422.
[14] I.M. Hsing, P. Futerko, Two-dimensional simulation of water transport in polymer electrolyte fuel cells, Chem. Eng. Sci. 55 (2000) 4209–4218.
[15] J.S. Yi, T.V. Nguyen, An along-the-channel model for proton exchange membrane fuel cells, J. Electrochem. Soc. 145 (1998) 1149–1159.
[16] L.R. Jordan, A.K. Shukla, T. Behrsing, N.R. Avery, B.C. Muddle, M. Forsyth, Diffusion layer parameters influencing optimal fuel cell performance, J. Power Sources 86 (2000) 250–254.
[17] L.R. Jordan, A.K. Shukla, T. Behrsing, N.R. Avery, B.C. Muddle, M. Forsyth, Effect of diffusion-layer morphology on the performance of polymer electrolyte fuel cells operating at atmospheric pressure, J. Appl. Electrochem. 30 (2000) 641–646.
[18] H.K. Lee, J.H. Park, D.Y. Kim, T.H. Lee, A study on the characteristics of the diffusion layer thickness and porosity of the PEMFC, J. Power Sources 131 (2004) 200–206.
[19] V. Gurau, F. Barbir, H. Liu, An analytical solution of a half-cell model for PEM fuel cells, J. Electrochem. Soc. 147 (2000) 2468–2477.
[20] H.S. Chu, C. Yeh, F. Chen, Effects of porosity change of gas diffuser on performance of proton exchange membrane fuel cell, J. Power Sources 123 (2003) 1–9.
[21] D. Natarajan, T.V. Nguyen, A two-dimensional, two-phase, multi-component, transient model for the cathode of a proton exchange membrane fuel cell using conventional gas distributors, J. Electrochem. Soc. 148 (2001) 1324–1335.
[22] T.V. Nguyen, R.E. White, A water and heat management model for proton-exchange-membrane fuel cells, J. Electrochem. Soc. 140 (1993) 2178–2186.
[23] J.J. Baschuk, X. Li, Modeling of polymer electrolyte membrane fuel cells with variable degrees of water flooding, J. Power Sources 86 (2000) 181–196.
[24] Z.H. Wang, C.Y. Wang, K.S. Chen, Two-phase flow and transport in the air cathode of proton exchange membrane fuel cells, J. Power Sources 94 (2001) 40–50.
[25] S.H. Ge, B.L. Yi, A mathematical model for PEMFC in different flow modes, J. Power Sources 124 (2003) 1–11.
[26] F.A.L. Dullien, Porous Media, Academic Press, New York, 1991.
[27] D.M. Bernardi, M.W. Verbrugge, Mathematical model of a gas diffusion electrode bonded to a polymer electrolyte, AIChE J. 37 (1991) 1151–1163.
[28] S. Mazumder, J.V. Cole, Rigorous 3-D mathematical modeling of PEM fuel cells II. Model predictions with liquid water transport, J. Electrochem. Soc. 150 (2003) A1510–A1517.
[29] T.E. Springer, T.A. Zawodizinski, S. Gottesfeld, Polymer electrolyte fuel cell model, J. Electrochem. Soc. 138 (1991) 2334–2342.